PHYSICAL REVIEW C **81**, 034316 (2010)

Microscopic description of spherical to γ-soft shape transitions in Ba and Xe nuclei

Z. P. Li,[1,2] T. Nikšić,[2] D. Vretenar,[2,*] and J. Meng[1,3]

[1]*State Key Laboratory of Nuclear Physics and Technology, School of Physics, Peking University, Beijing 100871, People's Republic of China*

[2]*Physics Department, Faculty of Science, University of Zagreb, 10000 Zagreb, Croatia*

[3]*School of Physics and Nuclear Energy Engineering, Beihang University, Beijing 100191, People's Republic of China*

(Received 8 February 2010; published 29 March 2010)

The rapid transition between spherical and γ-soft shapes in Ba and Xe nuclei in the mass region $A \geqslant 130$ is analyzed using excitation spectra and collective wave functions obtained by diagonalization of a five-dimensional Hamiltonian for quadrupole vibrational and rotational degrees of freedom, with parameters determined by constrained self-consistent relativistic mean-field calculations for triaxial shapes. The results reproduce the characteristic evolution of excitation spectra and E2 transition probabilities, and in general, a good agreement with available data is obtained. The calculated spectra display fingerprints of a second-order shape phase transition that can approximately be described by analytic solutions corresponding to the E(5) dynamical symmetry.

DOI: 10.1103/PhysRevC.81.034316 PACS number(s): 21.60.Jz, 21.60.Ev, 21.10.Re, 21.90.+f

I. INTRODUCTION

Atomic nuclei display a variety of equilibrium shapes—spherical, axially deformed shapes that are soft with respect to triaxial deformations. In most cases the transitions between different shapes in isotopic or isotonic sequences are gradual and reflect the underlying modifications of single-nucleon shell structure and interactions between valence nucleons. In a number of cases, however, with the addition or subtraction of only a few nucleons, one finds experimental signatures of abrupt changes in observables that characterize ground-state nuclear shapes. In the last decade the concept of quantum phase transitions (QPTs) has successfully been applied and investigated, both experimentally and theoretically, in equilibrium shape changes of nuclei [1–6].

The two best-studied classes of nuclear shape phase transitions correspond to a second-order QPT between spherical and γ-soft shapes [7,8] and a first-order QPT between spherical and axially deformed shapes [9,10]. Most theoretical studies of QPT in nuclei have been based on model specific Hamiltonians that, by construction, describe shape changes, that is, a phase transition is accessed by variation of a control parameter explicitly built into the Hamiltonian. For instance, a QPT can be described in the geometric framework in terms of a Bohr Hamiltonian for shape variables and related to the concept of critical symmetries that provide parameter independent predictions for excitation spectra and electric quadrupole (E2) transition rates for nuclei at the phase transition point. Analytic solutions of the eigenvalue problem at the critical point are associated with zeros of special functions. Alternatively, in the algebraic approach different shapes coincide with particular dynamic symmetries of some algebraic structure, and a QPT may occur when these symmetries are broken in a specific way. An example of the latter approach is the framework of the interacting-boson model [11] and its various extensions.

More recently a number of studies have appeared that attempt a fully microscopic description of shape QPT starting from nucleonic degrees of freedom [12–20]. An approach in terms of explicit nucleonic degrees of freedom is particularly important because the physical control parameter in a nuclear QPT is the actual number of nucleons. In a series of studies [15,19,20] we investigated nuclear QPT in the region $Z = 60, 62, 64$, with $N \approx 90$, using a microscopic approach based on constrained self-consistent relativistic mean-field calculations of potential energy surfaces. Because a quantitative analysis of QPT must go beyond a simple mean-field level, that is, one must be able to calculate ratios of excitation energies and electromagnetic transition rates, in Ref. [15] the generator coordinate method was used to perform configuration mixing of angular-momentum and particle-number projected relativistic wave functions restricted to axial symmetry. This approach was extended in Refs. [19] and [20], where collective excitation spectra and transition probabilities were calculated starting from a five-dimensional Hamiltonian for quadrupole vibrational and rotational degrees of freedom, with parameters determined by constrained mean-field calculations for triaxial shapes, that is, including both β and γ deformations. The results reproduced available data and showed that there is an abrupt change of structure at $N = 90$ that can be characterized approximately by the $X(5)$ analytic solution [9] at the critical point of the first-order quantum phase transition between spherical and axially deformed shapes. As a function of the physical control parameter, the number of nucleons, energy gaps between the ground state and the excited vibrational states with zero angular momentum, isomer shifts, and monopole transition strength exhibit sharp discontinuities at neutron number $N = 90$, characteristic of a first-order quantum phase transition.

Are the remarkable results for $X(5)$-like shape phase transitions in the mass region $A \approx 150$ [15,19,20] somewhat accidental? Can the same universal energy density functional describe other types of shape phase transitions, and in different regions of the chart of nuclides? To answer these questions we apply the same model to the study of γ-soft shapes in Ba and Xe nuclei in the mass $A \geqslant 130$ region, where evidence has been reported for a second-order QPT between spherical and γ-soft shapes. This is a phase transition in one degree of

*vretenar@physik.tu-muenchen.de

freedom—the axial deformation β—and, in the interacting-boson model language, represents a transition between the $U(5)$ and the $O(6)$ dynamical symmetries in the limit of a large boson number. The critical point of phase transition can also be related to a dynamical symmetry, in this case $E(5)$ [7], and the experimental realization of this critical-point symmetry was first identified in the spectrum of ^{134}Ba [8].

The model is based on constrained self-consistent relativistic mean-field calculations for triaxial shapes, that is, including both β and γ deformations. The resulting self-consistent solutions—single-particle wave functions, occupation probabilities, and quasiparticle energies that correspond to each point on the binding energy surface—are used to calculate the parameters that determine the collective Hamiltonian: three mass parameters, three moments of inertia, and the zero-point energy corrections, as functions of the deformations β and γ [21]. The diagonalization of the Hamiltonian yields the excitation energies and collective wave functions that are used to calculate observables. No attempt is made to tune the model or the parameters to this particular type of shape transition or mass region. As in our previous studies of $X(5)$-like transitions [15,19,20], the relativistic functional PC-F1 (point-coupling Lagrangian) [22] is used in the particle-hole channel, and a density-independent δ force is the effective interaction in the particle-particle channel, with pairing correlations treated in the BCS approximation.

II. SHAPE TRANSITION IN Ba AND Xe ISOTOPES

Our analysis starts with the self-consistent relativistic mean-field plus BCS calculation of quadrupole energy surfaces of Ba and Xe isotopes. The map of the energy surface as a function of the quadrupole deformation is obtained by imposing constraints on the axial and triaxial mass quadrupole moments. The method of quadratic constraints uses an unrestricted variation of the function

$$\langle H\rangle + \sum_{\mu=0,2} C_{2\mu}(\langle\hat{Q}_{2\mu}\rangle - q_{2\mu})^2, \tag{1}$$

where $\langle H\rangle$ is the total energy, and $\langle\hat{Q}_{2\mu}\rangle$ denotes the expectation value of the mass quadrupole operators:

$$\hat{Q}_{20} = 2z^2 - x^2 - y^2 \quad \text{and} \quad \hat{Q}_{22} = x^2 - y^2. \tag{2}$$

$q_{2\mu}$ is the constrained value of the multipole moment, and $C_{2\mu}$ the corresponding stiffness constant [23].

In Fig. 1 we display the RMF + BCS triaxial quadrupole binding energy maps of the even-even $^{136\text{-}130}$Ba in the β-γ plane ($0 \leqslant \gamma \leqslant 60^\circ$). All energies are normalized with respect to the binding energy of the absolute minimum, and the contours join points on the surface with the same energy (in megaelectronvolts). For each nucleus in the corresponding inset we plot the axial projection of the binding energy for oblate (negative-β) and prolate (positive-β) deformations. The corresponding energy maps of the even-even $^{134\text{-}128}$Xe isotopes are shown in Fig. 2. Both for Ba and for Xe, these plots illustrate the rapid transition from spherical shapes near the $N = 82$ closed shell to γ-soft energy surfaces for lighter isotopes. Starting from almost-perfect spherical shapes in ^{136}Ba and ^{134}Xe, the decrease in neutron number induces quadrupole deformations. In the axial plots we note that the potentials become less stiff in β and that two minima develop, one prolate and one oblate, at almost the same energy and separated by a low spherical barrier. However, the three-dimensional energy maps show that the spherical

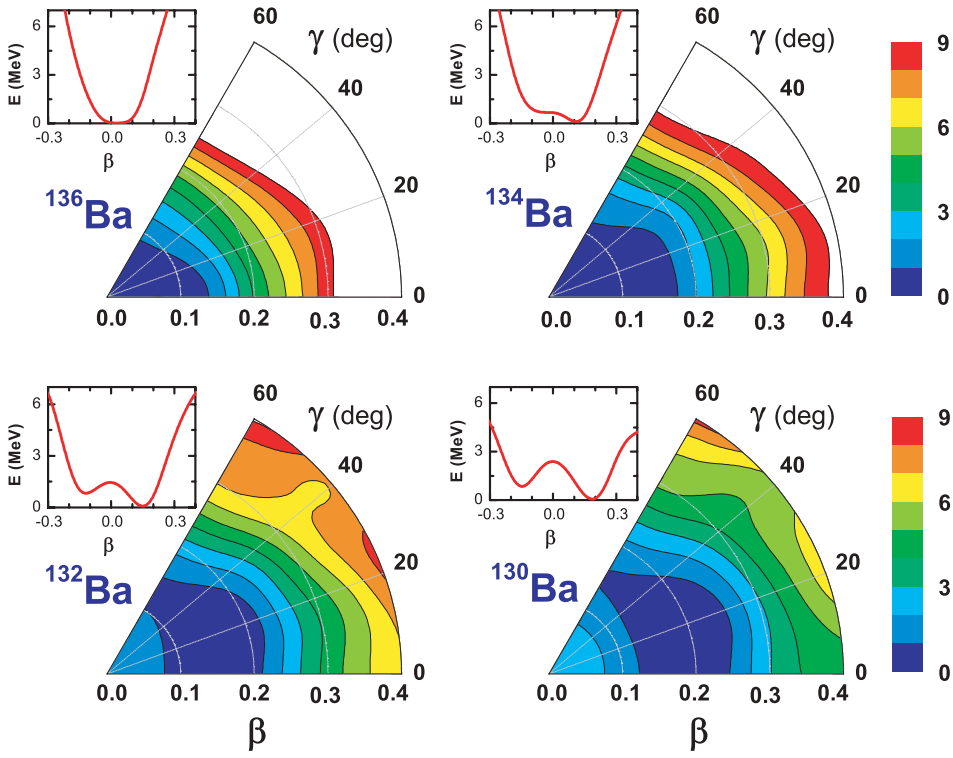

FIG. 1. (Color online) Self-consistent RMF + BCS triaxial quadrupole binding energy maps of the even-even $^{136\text{-}130}$Ba isotopes in the β-γ plane ($0 \leqslant \gamma \leqslant 60^\circ$). All energies are normalized with respect to the binding energy of the absolute minimum; the contours join points on the surface with the same energy (in megaelectronvolts). For each nucleus in the corresponding inset, we plot the axial projection of the binding energy for oblate (negative-β) and prolate (positive-β) deformations.

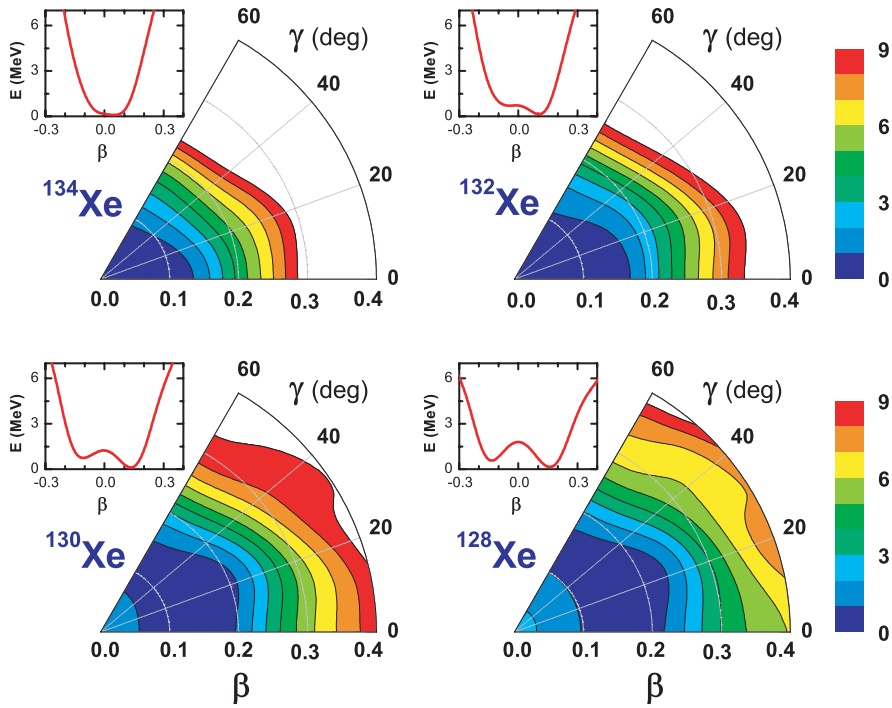

FIG. 2. (Color online) Same as Fig. 1, but for the isotopes $^{134\text{-}128}$Xe.

barriers are concentrated around $\beta \approx 0$, and therefore, rather than two separate minima, the potentials display continuous γ-soft minima that extend from prolate to oblate shapes.

Of particular interest in the present analysis are the nuclei that have been identified as possible candidates for a shape phase transition that can be characterized by the $E(5)$ dynamical symmetry [7]. The experimental realization of this critical-point symmetry, associated with a second-order quantum phase transition between spherical and γ-soft potential shapes, was first identified in ^{134}Ba [8]. $E(5)$ is the symmetry of a five-dimensional (intrinsic variables β and γ and the three Euler angles) infinite well in the axial deformation variable β [$V(\beta) = 0$ for $|\beta| \leqslant \beta_W$, and $V(\beta) = \infty$ for $|\beta| > \beta_W$], and the potential is completely γ independent. The microscopic binding energy curve $E(\beta)$ of ^{134}Ba (Fig. 1) displays a shape that is almost symmetric with respect to $\beta = 0$. One notes a relatively flat bottom between $\beta \approx -0.1$ and $\beta \approx 0.1$ (the oblate configuration is only $\approx$0.5 MeV above the prolate minimum), and the potential is rather stiff for $|\beta| > 0.15$. The dependence on the triaxial deformation parameter γ is shown in the corresponding three-dimensional energy map and, even more clearly, in Fig. 3, where we plot the binding energy curves as functions of γ for several values of axial deformation: $\beta = 0.05$, 0.1, 0.15, and 0.2. In the region of the flat bottom $|\beta| \leqslant 0.1$ the binding energy of ^{134}Ba is indeed almost independent of γ, and even for somewhat larger deformations, $0.1 \leqslant |\beta| \leqslant 0.2$, only a weak dependence on γ is predicted by the calculation based on the PC-F1 functional. A very similar energy surface is calculated for the isotone ^{132}Xe (Figs. 2 and 4).

In the next step the constrained self-consistent solutions of the relativistic mean-field plus BCS equations, that is, the single-particle wave functions, occupation probabilities, and quasiparticle energies that correspond to each point on the binding energy surfaces in Figs. 1 and 2, are used to calculate the parameters that determine the collective Hamiltonian [21],

$$\hat{H} = \hat{T}_{\text{vib}} + \hat{T}_{\text{rot}} + V_{\text{coll}}, \tag{3}$$

with the vibrational kinetic energy,

$$\hat{T}_{\text{vib}} = -\frac{\hbar^2}{2\sqrt{wr}} \left\{ \frac{1}{\beta^4} \left[\frac{\partial}{\partial\beta} \sqrt{\frac{r}{w}} \beta^4 B_{\gamma\gamma} \frac{\partial}{\partial\beta} - \frac{\partial}{\partial\beta} \sqrt{\frac{r}{w}} \beta^3 B_{\beta\gamma} \frac{\partial}{\partial\gamma} \right] + \frac{1}{\beta \sin 3\gamma} \left[-\frac{\partial}{\partial\gamma} \sqrt{\frac{r}{w}} \sin 3\gamma \times B_{\beta\gamma} \frac{\partial}{\partial\beta} + \frac{1}{\beta} \frac{\partial}{\partial\gamma} \sqrt{\frac{r}{w}} \sin 3\gamma B_{\beta\beta} \frac{\partial}{\partial\gamma} \right] \right\}, \tag{4}$$

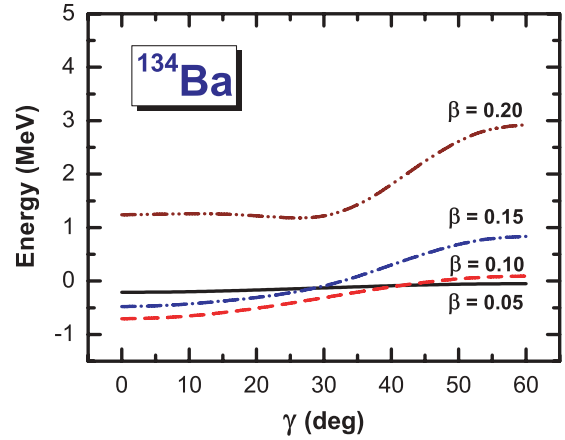

FIG. 3. (Color online) Self-consistent RMF + BCS binding energy curves of the ^{134}Ba nucleus, as functions of the deformation parameter γ, for four values of axial deformation, $\beta = 0.05$, 0.1, 0.15, and 0.2.

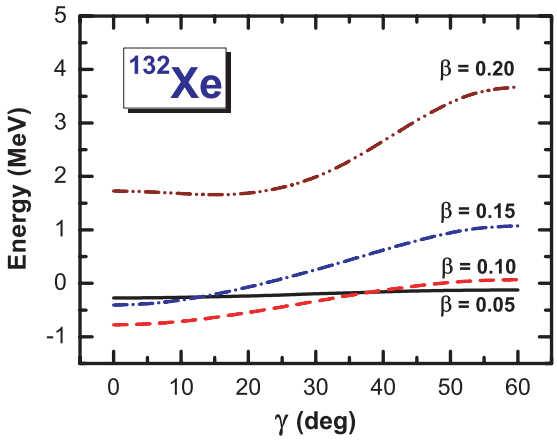

FIG. 4. (Color online) Same as Fig. 3, but for the ^{132}Xe nucleus.

and rotational kinetic energy,

$$\hat{T}_{\rm rot} = \frac{1}{2}\sum_{k=1}^{3}\frac{\hat{J}_k^2}{\mathcal{I}_k}. \tag{5}$$

$V_{\rm coll}$ is the collective potential. $\hat{J}_k$ denotes the components of the angular momentum in the body-fixed frame of a nucleus, and the mass parameters $B_{\beta\beta}$, $B_{\beta\gamma}$, and $B_{\gamma\gamma}$, as well as the moments of inertia $\mathcal{I}_k$, depend on the quadrupole deformation variables β and γ:

$$\mathcal{I}_k = 4B_k\beta^2\sin^2(\gamma - 2k\pi/3). \tag{6}$$

Two additional quantities that appear in the expression for the vibrational energy, $r = B_1B_2B_3$ and $w = B_{\beta\beta}B_{\gamma\gamma} - B_{\beta\gamma}^2$, determine the volume element in the collective space. The moments of inertia are calculated from the Inglis-Belyaev (IB) formula:

$$\mathcal{I}_k = \sum_{i,j}\frac{(u_iv_j - v_iu_j)^2}{E_i + E_j}\langle i|\hat{J}_k|j\rangle|^2, \quad k = 1, 2, 3, \tag{7}$$

where k denotes the axis of rotation, and the summation runs over the proton and neutron quasiparticle states. The mass parameters associated with the two quadrupole collective coordinates $q_0 = \langle\hat{Q}_{20}\rangle$ and $q_2 = \langle\hat{Q}_{22}\rangle$ are also calculated in the cranking approximation,

$$B_{\mu\nu}(q_0, q_2) = \frac{\hbar^2}{2}\left[\mathcal{M}_{(1)}^{-1}\mathcal{M}_{(3)}\mathcal{M}_{(1)}^{-1}\right]_{\mu\nu}, \tag{8}$$

with

$$\mathcal{M}_{(n),\mu\nu}(q_0, q_2) = \sum_{i,j}\frac{\langle i|\hat{Q}_{2\mu}|j\rangle\langle j|\hat{Q}_{2\nu}|i\rangle}{(E_i + E_j)^n}(u_iv_j + v_iu_j)^2. \tag{9}$$

Finally, the potential $V_{\rm coll}$ in the collective Hamiltonian Eq. (3) is obtained by subtracting the zero-point energy corrections from the total energy that corresponds to the solution of constrained RMF + BCS equations, at each point on the triaxial deformation plane.

The Hamiltonian, Eq. (3), describes quadrupole vibrations, rotations, and the coupling of these collective modes. The corresponding eigenvalue problem is solved using an expansion of eigenfunctions in terms of a complete set of basis functions that depend on the deformation variables β and γ and the Euler angles ϕ, θ, and ψ [21]. The diagonalization of the Hamiltonian yields the excitation energies and collective wave functions:

$$\Psi_\alpha^{IM}(\beta, \gamma, \Omega) = \sum_{K\in\Delta I}\psi_{\alpha K}^I(\beta, \gamma)\Phi_{MK}^I(\Omega). \tag{10}$$

The angular part corresponds to linear combinations of Wigner functions,

$$\Phi_{MK}^I(\Omega) = \sqrt{\frac{2I+1}{16\pi^2(1+\delta_{K0})}}\left[D_{MK}^{I*}(\Omega) + (-1)^I D_{M-K}^{I*}(\Omega)\right], \tag{11}$$

and the summation in Eq. (10) is over the allowed set of K values:

$$\Delta I = \begin{cases} 0, 2, \ldots, I & \text{for} \quad I \bmod 2 = 0, \\ 2, 4, \ldots, I-1, & \text{for} \quad I \bmod 2 = 1\,. \end{cases} \tag{12}$$

In Figs. 5 and 6 we plot the isotopic dependence of two characteristic collective observables, $R_{4/2}$ and B(E2; $2_1^+ \to 0_1^+$) (in Weisskopf units), for Ba and Xe nuclei, respectively. The values obtained by the diagonalization of the collective Hamiltonian, Eq. (3), with parameters determined by the microscopic relativistic energy density functional PC-F1, are shown in comparison with data [24,25]. For a transition between γ-soft rotors [$O(6)$ dynamical symmetry limit of the interacting boson model] and spherical vibrators [$U(5)$ dynamical symmetry limit], the ratio between the excitation energies of the first 4^+ and 2^+ states varies from the value $R_{4/2} = 2.5$ in the $O(6)$ limit, and $R_{4/2} = 2$ for a spherical vibrator. For a second-order shape phase transition between these limits, the parameter-free $E(5)$ symmetry prediction at the critical point is $R_{4/2} = 2.2$. The calculation reproduces the rapid decrease in $R_{4/2}$ with mass number. The agreement with the empirical ratios is somewhat better in the case of Ba isotopes, but even for Xe nuclei the differences are not large.

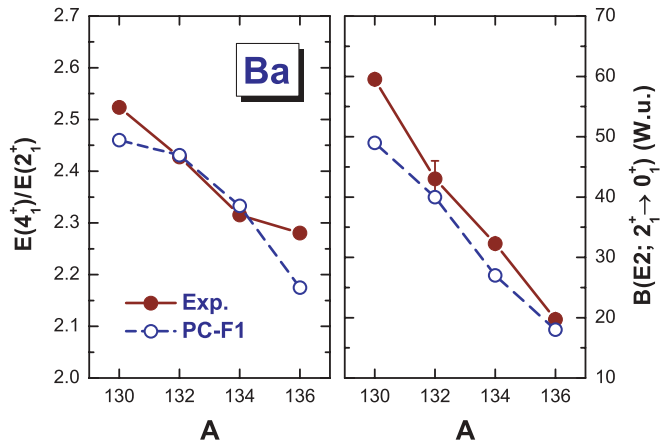

FIG. 5. (Color online) Evolution of the characteristic collective observables $R_{4/2}$ and B(E2; $2_1^+ \to 0_1^+$) (in Weisskopf units) with mass number in Ba isotopes. Microscopic values calculated with the PC-F1 energy density functional are shown in comparison with data [24,25].

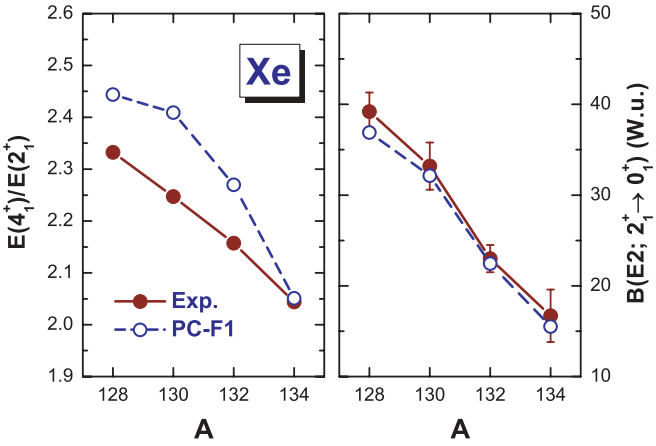

FIG. 6. (Color online) Same as Fig. 5, but for the isotopes $^{128\text{-}134}$Xe.

The largest deviation from the experimental value is calculated for ^{130}Xe ≈ 0.15. For the $N = 78$ isotones ^{134}Ba and ^{132}Xe, the calculated ratios $R_{4/2} \approx 2.3$ are not very different from the $E(5)$ symmetry prediction. An even better agreement with data is obtained for the calculated isotopic dependence of the transition probabilities $B(\mathrm{E2}; 2_1^+ \rightarrow 0_1^+)$ (Figs. 5 and 6, right). For instance, the calculation reproduces in detail the swift decrease in the empirical B(E2) values from ≈40 Weisskopf units in ^{128}Xe to ≈15 Weisskopf units in ^{134}Xe. It should be noted that the calculation is completely parameter-free; that is, physical observables, such as transition probabilities and spectroscopic quadrupole moments, are calculated in the full configuration space and there is no need for effective charges.

Before comparing the calculated excitation spectra and E2 transition rates with available data and $E(5)$ symmetry model predictions, in Figs. 7 and 8 we plot the relative fluctuations of the quadrupole deformations, $\Delta\beta/\langle\beta\rangle$ and $\Delta\gamma/\langle\gamma\rangle$, for the

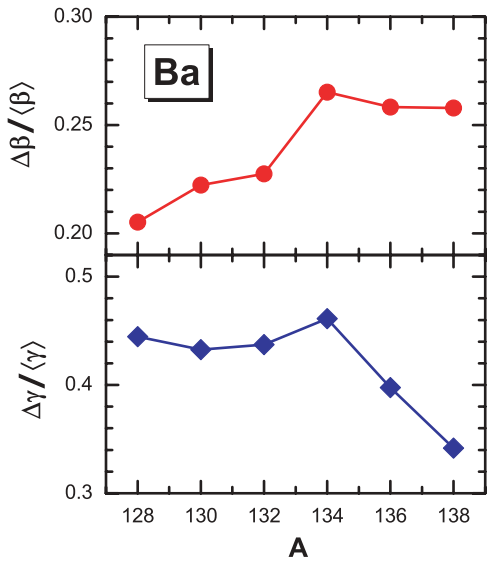

FIG. 7. (Color online) Fluctuations of the quadrupole deformations $\Delta\beta/\langle\beta\rangle$ and $\Delta\gamma/\langle\gamma\rangle$ for the sequence of ground states of Ba isotopes.

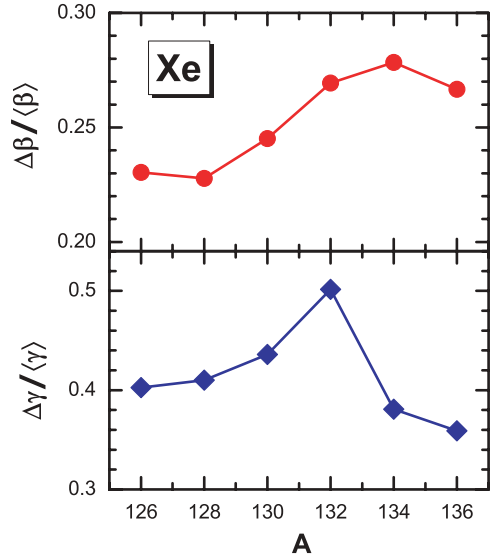

FIG. 8. (Color online) Same as Fig. 7, but for the isotopes of Xe.

sequence of ground states of Ba and Xe isotopes, respectively. The variances are defined by [26]

$$\Delta\beta = \sqrt{\langle\beta^4\rangle - \langle\beta^2\rangle^2}/2\langle\beta\rangle,$$
$$\Delta\gamma = \sqrt{\frac{\langle\beta^6\cos^2 3\gamma\rangle}{\langle\beta^6\rangle} - \frac{\langle\beta^3\cos 3\gamma\rangle^2}{\langle\beta^4\rangle\langle\beta^2\rangle}} \Big/ 3\sin(3\langle\gamma\rangle), \tag{13}$$

where the average values of β and γ,

$$\langle\beta\rangle = \sqrt{\langle\beta^2\rangle},$$
$$\langle\gamma\rangle = \arccos(\langle\beta^3\cos 3\gamma\rangle/\sqrt{\langle\beta^4\rangle\langle\beta^2\rangle})/3, \tag{14}$$

are calculated in the nuclear ground state, that is, in the lowest eigenstate of the collective Hamiltonian. It is interesting to note the change in the fluctuations around $N = 78$. For a transition from deformed to spherical shapes one expects an increase in the relative fluctuation $\Delta\beta/\langle\beta\rangle$. For the triaxial deformation variable γ the calculation predicts a marked maximum of the relative fluctuation in ^{134}Ba and ^{132}Xe, which can be interpreted as a possible fingerprint of the second-order shape phase transition.

^{134}Ba was the first nucleus to be considered as a good example of empirical realization of the $E(5)$ symmetry at the critical point of the second-order phase transition between spherical and γ-soft shapes [8]. In Fig. 9 we compare the spectrum of the collective Hamiltonian for ^{134}Ba with available data for positive-parity states [24,25,27,28] and with the predictions of the $E(5)$ model. For the moments of inertia of the collective Hamiltonian we have multiplied the IB values, Eq. (7), with a common factor determined in such a way that the calculated energy of the 2_1^+ state coincides with the experimental value [19,21]. This additional scale parameter is necessary because of the well-known fact that the IB formula, Eq. (7), predicts effective moments of inertia that are considerably smaller than empirical values. Following the minimal prescription in Ref. [29], the moments of inertia that parametrize the collective Hamiltonian can be simply related to the IB values: $\mathcal{I}_k(q) = \mathcal{I}_k^{IB}(q)(1+\alpha)$, where q denotes the

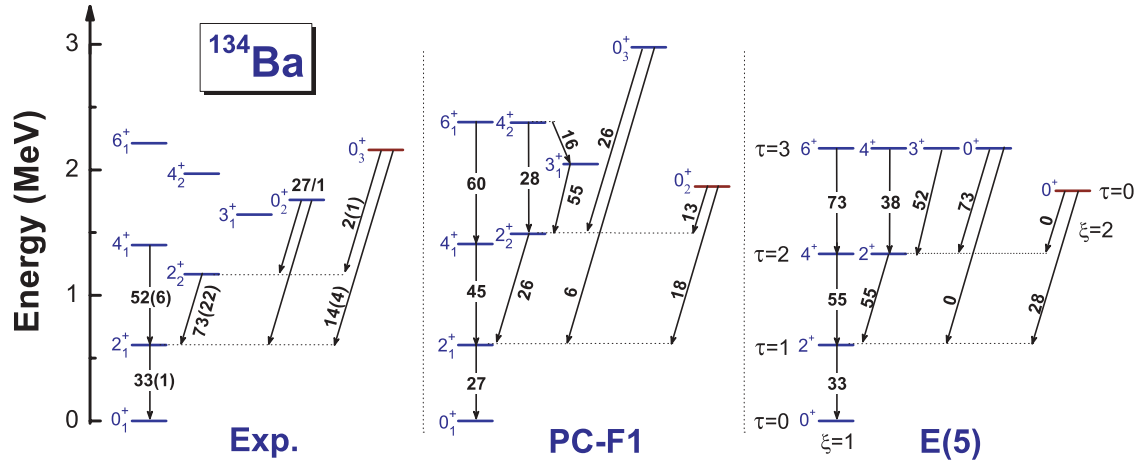

FIG. 9. (Color online) The low-energy spectrum of ^{134}Ba calculated with the PC-F1 relativistic density functional (middle), compared with the data (left), and the $E(5)$ symmetry predictions (right) for the excitation energies and intraband and interband B(E2) values (in Weisskopf units). Theoretical spectra are normalized to the experimental energy of state 2_1^+, and $E(5)$ transition strengths are normalized to the experimental $B(\mathrm{E2}; 2_1^+ \to 0_1^+)$.

generic deformation parameter, and α is a constant that can be determined in a comparison with data [19]. Here we discuss in more detail the approximations used in the calculation of moments of inertia and mass parameters.

The excitation spectrum of the collective Hamiltonian determined by the PC-F1 density functional is in good agreement with the available data. This is especially true for the excitation energies and transitions in the ground-state band. The calculated sequence of states 2_2^+, 3_1^+, and 4_2^+ is approximately 300 keV higher than the corresponding experimental levels, and the transition $2_2^+ \to 2_1^+$ is considerably weaker compared to experiment (note, however, the large error bar of the experimental value). By comparing the de-excitation pattern of the two excited 0^+ states, it appears that the ordering of these states is reversed in the theoretical spectrum. The calculation predicts that the second 0^+ state predominantly decays to 2_1^+, and for the third 0^+ state a much stronger transition to 2_2^+ is predicted. In fact, the calculated 0_2^+ state is close in energy to the experimental 0_3^+ state, which displays a similar E2 branching to 2_1^+ and 2_2^+. The third theoretical 0^+ state, however, is calculated more than 1 MeV above the corresponding experimental 0_2^+ state. One might also note that the absolute B(E2) values (in Weisskopf units) for the stronger transitions are in very good agreement with data, but the calculated 0_2^+ and 0_3^+ states are obviously much more mixed than the corresponding experimental states. This also explains the strong repulsion between the theoretical second and third 0^+ states.

It is interesting to compare the PC-F1 excitation spectrum with the $E(5)$ level scheme that corresponds to ^{134}Ba (Fig. 9, right). In addition to the total angular momentum I, in the case of $E(5)$ symmetry states are labeled by two quantum numbers: $\xi = 1, 2, 3, \ldots$ enumerates the zeros of the Bessel functions $J_{\tau+(3/2)}$ in β, and $\tau = 0, 1, 2, \ldots$ is associated with the $O(5)$ algebra and denotes the phononlike levels within a ξ family [7]. The corresponding spectrum is parameter-free up to an overall scale factor that is adjusted by normalizing the energies to the experimental excitation energy of the first excited state 2_1^+. The $E(5)$ transition rates are normalized to the experimental $B(\mathrm{E2}; 2_1^+ \to 0_1^+)$. Some striking similarities are found in the comparison of PC-F1 and $E(5)$ excitation spectra for ^{134}Ba. For instance, in the ground-state band the calculated ratios,

$$R_1 = \frac{B(\mathrm{E2}; 4_1^+ \to 2_1^+)}{B(\mathrm{E2}; 2_1^+ \to 0_1^+)} = 1.67$$

$$\text{and} \quad R_2 = \frac{B(\mathrm{E2}; 6_1^+ \to 4_1^+)}{B(\mathrm{E2}; 4_1^+ \to 2_1^+)} = 1.33,$$

exactly coincide with the values predicted by the $E(5)$ symmetry model. Again, we emphasize that the calculation of transition probabilities in the microscopic collective model is parameter-free. A very good agreement is also found for $B(\mathrm{E2}; 4_2^+ \to 2_2^+)$ and $B(\mathrm{E2}; 3_1^+ \to 2_2^+)$. The second 0^+ state is calculated at an excitation energy very close to the predicted position of $0^+_{\xi=2,\tau=0}$, and this state also predominantly decays to 2_1^+ [$\Delta\tau = 1$ transition in the $E(5)$ model]. Even though calculated at a much higher energy, the decay pattern of the third 0^+ state is similar to that of the third $E(5)$ 0^+ state with $\xi = 1$ and $\tau = 3$. The two excited 0^+ states in the $E(5)$ model belong to different ξ multiplets, and only $\Delta\tau = 1$ transitions are allowed. The microscopic collective Hamiltonian, on the contrary, breaks the symmetry and this is reflected in both the decay pattern and the excitation energy of the 0_3^+ state. Another difference between the PC-F1 and the $E(5)$ spectrum is the transition $2_2^+ \to 2_1^+$, for which the $E(5)$ model predicts the same B(E2) value as for $4_1^+ \to 2_1^+$. The smaller value calculated from the eigenvectors of the collective Hamiltonian can be understood by considering the corresponding probability density distributions. For a given collective state Eq. (10), the probability density distribution in the (β, γ) plane is defined by

$$\rho_{I\alpha}(\beta, \gamma) = \sum_{K \in \Delta I} \left|\psi^I_{\alpha K}(\beta, \gamma)\right|^2 \beta^3 |\sin 3\gamma|. \qquad (15)$$

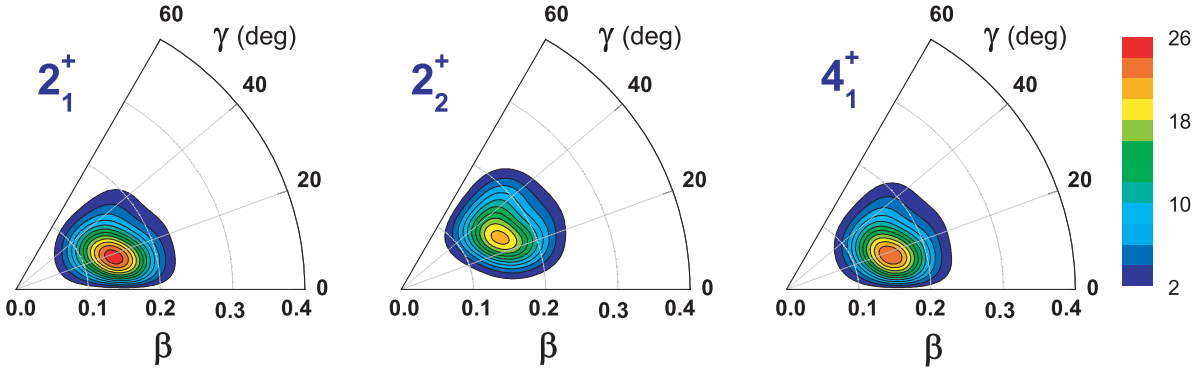

FIG. 10. (Color online) Probability densities, Eq. (15), in the β-γ plane for states 2_1^+, 2_2^+, and 4_1^+ of ^{134}Ba.

The normalization reads

$$\int_0^\infty \beta d\beta \int_0^{2\pi} d\gamma \; \rho_{I\alpha}(\beta,\gamma) = 1. \tag{16}$$

In Fig. 10 we plot the probability densities in the β-γ plane for states 2_1^+, 2_2^+, and 4_1^+ of ^{134}Ba. States 2_1^+ and 4_1^+ belong to the ground-state band, and the corresponding wave functions display a large overlap in the β-γ plane. The average values of β are 0.156 for 2_1^+ and 0.166 for 4_1^+, respectively, and the average values of γ are 23.4^0 for 2_1^+ and 23.7^0 for 4_1^+. Because of the large overlap of the wave functions, one expects a strong transition between these states. For state 2_2^+ the average value of of β is 0.174, but $\langle\gamma\rangle = 29.6^0$; that is, the overlap between the collective wave functions of states 2_1^+ and 2_2^+ is smaller than that between 2_1^+ and 4_1^+. Consequently, the transition $2_2^+ \to 2_1^+$ is weaker than $4_1^+ \to 2_1^+$. However, as already noted, this result is not in agreement with data showing that the transition $2_2^+ \to 2_1^+$ is in fact stronger than $4_1^+ \to 2_1^+$.

Turning now to the sequence of Xe isotopes, in Fig. 11 the PC-F1 collective excitation spectrum of ^{132}Xe, that is, the isotone of ^{134}Ba, is compared with available data [24,30] and the level scheme predicted by the $E(5)$ symmetry model. We find reasonable agreement with experiment and, again, a remarkable similarity with the decay pattern predicted for the $E(5)$ critical-point symmetry. The limited set of data, however, does not provide strong evidence for ^{132}Xe being a good example of empirical realization of the $E(5)$ critical-point symmetry. Therefore in Fig. 12 we also display the spectra of ^{130}Xe. In this case the microscopic calculation based on the PC-F1 functional predicts an excitation spectrum in slightly better agreement with available data [24,30], for example, the transitions between low-lying states, and the decay scheme is also very similar to the one that characterizes the $E(5)$ symmetry, except for a weaker transition $2_2^+ \to 2_1^+$, which has already been discussed in the case of ^{134}Ba. One might even note that the calculated E2 transitions from 0_2^+ and 0_3^+ are, for this nucleus, actually closer to the branching pattern predicted by $E(5)$ than they were in the case of ^{134}Ba and ^{132}Xe. The transitions $0_3^+ \to 2_1^+$ and $0_2^+ \to 2_2^+$, which are forbidden in the $E(5)$ symmetry limit because of the $\Delta\tau = 1$ selection rule, are strongly suppressed between eigenstates of the PC-F1-based collective Hamiltonian.

In a systematic search for experimental fingerprints of $E(5)$ critical-point symmetry [31], it was suggested that one possible candidate might be ^{128}Xe. However, for this nucleus the ratio $R_{4/2} = 2.33$ is intermediate between the value for $E(5)$ ($R_{4/2} = 2.2$) and the deformed γ-independent limit or $O(6)$ ($R_{4/2} = 2.5$). In fact, the microscopic potential of ^{128}Xe (Fig. 2) displays a γ-independent surface for axial deformations $0.1 \leqslant \beta \leqslant 0.2$. We also notice that the potential is not nearly as rigid in β for $\beta \leqslant 0.1$ and $\beta > 0.2$, as one assumes in the $E(5)$ symmetry limit. In Ref. [32] a γ-soft

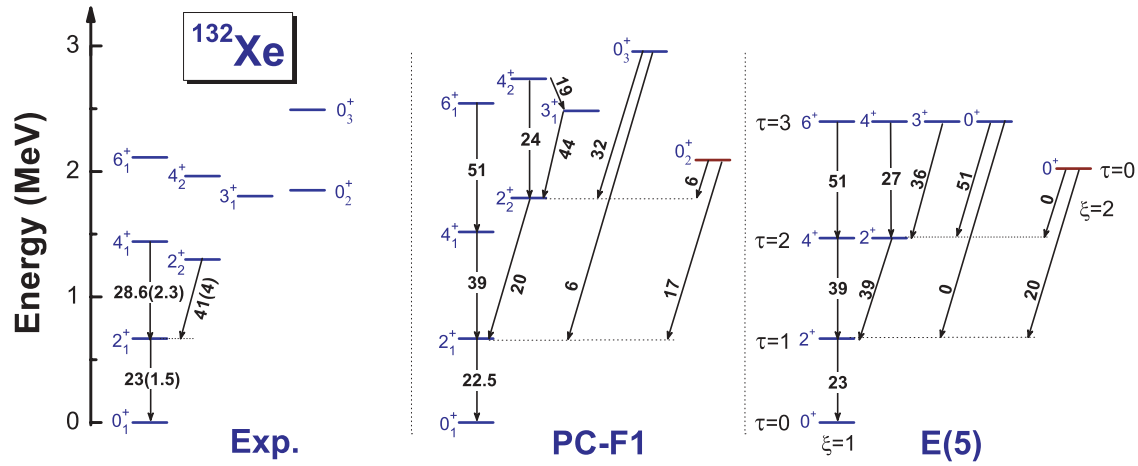

FIG. 11. (Color online) Same as Fig. 9, but for the ^{132}Xe nucleus.

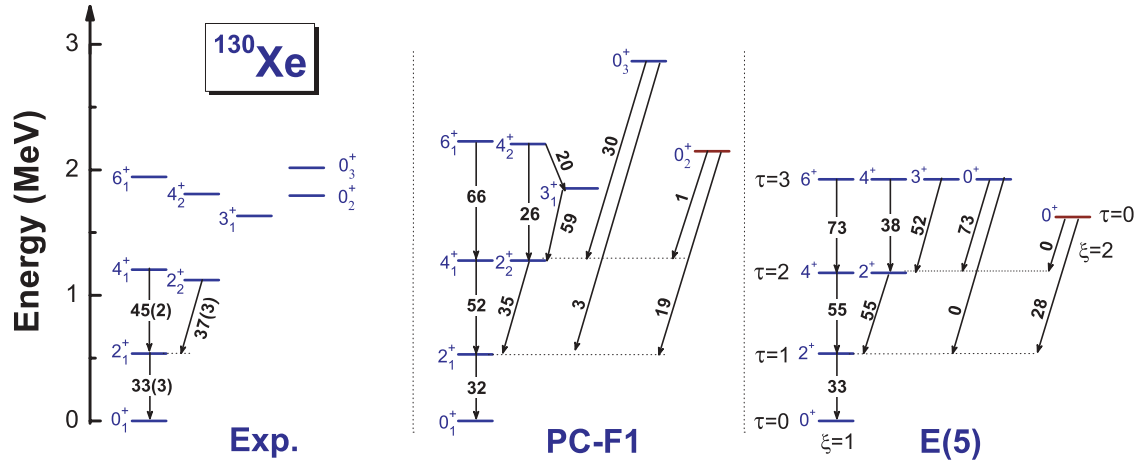

FIG. 12. (Color online) Same as Fig. 9 but for the ^{130}Xe nucleus.

analog of the confined β-soft (CBS) rotor model [33] has been constructed, that corresponds to an infinite square-well potential over a confined range of values $\beta_M > \beta_m \geqslant 0$ (confined β-soft potential, β_m and β_M denote the positions of the inner and outer walls on the β axis, respectively). The γ-soft extension of Ref. [32] generalizes the $E(5)$ critical-point symmetry to a parametric solution over the whole path between $E(5)$ and the β-rigid deformed γ-independent limit. The structure of ^{128}Xe was investigated and, from the decay pattern of the first two excited 0^+ states, it was suggested that ^{128}Xe is located well beyond the $U(5) \rightarrow O(6)$ shape-phase transition in the deformed phase. In a very recent experimental study of low-lying collective states in ^{128}Xe by γ-ray spectroscopy [34], the data, including the first measurement of the B(E2) values for transitions from the 0_2^+ and 0_3^+ states, were compared with theoretical predictions and it was concluded that ^{128}Xe is not an $E(5)$ nucleus, thus leaving ^{130}Xe as the best candidate among the Xe isotopes. In Fig. 13 we, therefore, finally compare our microscopic results for ^{128}Xe with the recent experimental decay scheme of Ref. [34]. The calculated excitation energies and B(E2) values for the ground-state band and the sequence 2_2^+, 3_1^+, 4_2^+ are in good agreement with experiment. The two excited 0^+ states, however, are calculated at a higher energy, especially 0_3^+. The predicted transitions to 2_1^+ and 2_2^+ clearly

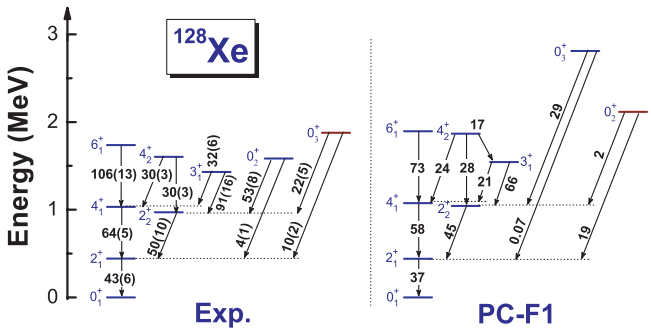

FIG. 13. (Color online) Experimental low-energy spectrum of ^{128}Xe (left), compared with the level scheme and decay pattern predicted by the solution of the microscopic collective Hamiltonian with the PC-F1 relativistic density functional.

follow the pattern calculated in ^{132}Xe and ^{130}Xe and do not reproduce the empirical two-level mixing that strongly breaks the $\Delta\tau = 1$ selection rule characteristic of $O(5)$ symmetry.

For all nuclei analyzed in this work we have found a very good agreement between data and the predictions of the microscopic collective Hamiltonian based on the PC-F1 energy density functional plus δ-force pairing, except for the two excited 0^+ states. In particular, the second excited 0^+ state, that is, the one that predominantly decays to 2_2^+, is systematically calculated at a considerably higher excitation energy compared to the experimental position of the two excited 0^+ levels. In ^{134}Ba and ^{128}Xe, for which data on absolute E2 transition strengths are available, it is the first excited 0^+ state that predominantly decays to 2_2^+, contrary to the results of our calculation. One reason for this discrepancy, of course, could be the particular choice of the energy density functional and/or the treatment of pairing correlations, but also the approximation used in the calculation of the mass parameters (vibrational inertial functions). In the current version of the model the moments of inertia are calculated from the IB formula [Eq. (7)]. These moments of inertia do not include the Thouless-Valatin dynamical rearrangement contributions and, therefore, are systematically smaller than the empirical values. However, as shown in several studies [29], the Thouless-Valatin corrections are almost independent of deformation, and the effective moments of inertia to be used in the collective Hamiltonian can simply be obtained by renormalizing the IB values by a constant factor, characteristic for a given nucleus. The situation is considerably more complicated in the case of mass parameters [35,36], for which there are no simple estimates of the Thouless-Valatin correction, especially for nuclei with γ-soft potential energy surfaces. Some authors [36] argue that, to approximately take into account the Thouless-Valatin correction, all inertial functions, not just the moments of inertia, should be rescaled by a constant multiplicative factor.

Another effect that is not included in our model is the coupling of nuclear shape oscillations with pairing vibrations, that is, vibrations of the pairing density. A number of studies have shown that excited 0^+ states are very sensitive to the coupling between these modes. For the Ba and Xe isotopes,

in particular, the effect of coupling between pairing vibrations and axial quadrupole vibrations was investigated in Ref. [37], using collective Hamiltonians based on a microscopic Nilsson single-particle Hamiltonian with pairing forces and a long-range residual interaction. It was shown that the coupling between the pairing and the quadrupole modes has a very pronounced effect on the lowest excited 0^+ states, lowering their excitation energies by 40%–50%, in much closer agreement with the data. In an even earlier study of collective states in Xe and Ba isotopes [38], based on the general five-dimensional Bohr Hamiltonian, this coupling was not taken into account explicitly, but rather it was simulated by a reduction of the pairing strengths of ≈20%. Even though the resulting pairing interaction is somewhat unphysical, that is, it gives proton and neutron gaps that are too small, the resulting excitation energies of the lowest 0^+ states are 40%–50% lower, in better agreement with experiment.

The present study, however, employs exactly the same model that was used in our previous analysis of spherical to axially deformed shape transitions. The mass parameters are calculated in the cranking approximation, Eqs. (8) and (9), and from these expressions it is obvious that the resulting mass parameters will be very sensitive to the underlying microscopic shell structure and to the treatment of pairing correlations. In fact, we have found that the position of the first excited 0^+ state in our calculation (the one that predominantly decays to 2_1^+) is sensitive to the value of the mass parameter $B_{\beta\beta}$, the excitation energy of the third 0^+ state (predominantly decaying to 2_2^+) displays a very strong dependence on $B_{\gamma\gamma}$, and the mixing of the two excited 0^+ states is controlled by $B_{\beta\gamma}$. For instance, by decreasing $B_{\beta\gamma}$, that is, by reducing the coupling between β and γ vibrational degrees of freedom, the mixing between 0_2^+ and 0_3^+ decreases and the resulting spectrum is even closer to the $E(5)$ level scheme. By increasing the value of $B_{\gamma\gamma}$ one finds a rapid decrease in the excited energy of the calculated 0_3^+, and eventually the two excited 0^+ state cross, in better agreement with available data for ^{134}Ba and ^{128}Xe. The only other effect on the calculated spectrum is a much smaller lowering of the sequence, 2_2^+, 3_1^+, 4_2^+, again in agreement with experiment. In the case of ^{128}Xe, for instance, an enhancement of $B_{\gamma\gamma}$ by a factor $\geqslant$1.5 brings the calculated excitation energies into very good agreement with the experimental spectrum shown in Fig. 13 [34].

Very recently a global study of low-energy nuclear structure at normal deformation has been reported, based on the nonrelativistic Hartree-Fock-Bogoliubov framework with the Gogny interaction D1S, and mapped onto a five-dimensional collective quadrupole Hamiltonian [39]. Ground-state properties, excitation energies, and quadrupole and monopole transition matrix elements for yrast levels up to 6_1^+ and the lowest yrare levels have been calculated for even-even particle-stable nuclei with proton numbers $Z = 10$ to $Z = 110$ and neutron number $N \leqslant 200$. Except for the use of a different effective interaction in the particle-hole and particle-particle channels, the model in Ref. [39] is very similar to the one employed in the present study. However, while in both models the quadrupole mass parameters are calculated in the cranking approximations, in the calculation of the moment of inertia the model in Ref. [39] goes beyond the simple IB formula used in this study and explicitly includes the Thouless-Valatin dynamical rearrangement contributions. This leads to an increase in the moments of inertia, and the resulting excitation energies of yrast states in deformed and transitional nuclei are, in general, in very good agreement with data. As a particular example, the study in Ref. [39] considered the low-energy collective quadrupole spectrum of ^{152}Sm. It was shown that the spectrum calculated with the collective Hamiltonian based on the Gogny interaction D1S is consistent with the $X(5)$ analytical solution at the critical point of QPT between spherical and axially deformed shapes in $N \approx 90$ isotones. More generally, the calculated spectral properties of ≈1700 even-even nuclei have demonstrated the predictive power of the quadrupole collective Hamiltonian model based on a microscopic effective interaction. A problem common to both studies, that is, to the global survey in Ref. [39] and the specific calculation of transitional Ba and Xe isotopes reported in this work, is the excitation energies of excited 0^+ states, which are systematically calculated too high compared with the data. Similar to the preceding discussion, in Ref. [39] it was suggested that the energies of excited 0^+ states could be improved by including the Thouless-Valatin dynamical rearrangement contributions in the calculation of the quadrupole mass parameters and by extending the model space to include two-quasiparticle components in the wave functions.

III. CONCLUSIONS

The recently developed implementation for the solution of the five-dimensional collective Hamiltonian for quadrupole vibrational and rotational degrees of freedom, with parameters determined by constrained self-consistent relativistic mean-field calculations for triaxial shapes, has been applied to the study of γ-soft shapes in Ba and Xe nuclei in the mass $A \geqslant 130$ region. This microscopic approach had previously been used to describe spherical to axially deformed shape transitions in the mass $A \approx 150$ region, and the results have shown that there is an abrupt change of structure at $N = 90$ that can approximately be characterized by the $X(5)$ analytic solution at the critical point of a first-order quantum phase transition. In this sense the present analysis represents a natural extension of our previous studies [15,19,20] to a region of nuclei where evidence has been reported for a second-order QPT between spherical and γ-soft shapes, with the critical point of phase transition characterized by the $E(5)$ dynamical symmetry. Without any modification of the model Hamiltonian, the treatment of pairing correlations, or the parameters of the effective interactions in the particle-hole and particle-particle channels, we have been able to describe the rapid transition between spherical and γ-soft shapes in Ba and Xe isotopes. The results reproduce the characteristic evolution of excitation spectra and E2 transition probabilities, and a good agreement with available data is obtained. In specific nuclei, for example, ^{134}Ba and ^{132}Xe, the calculated triaxial quadrupole binding energy surfaces are rather flat in an extended interval of the axial deformation parameter β and almost independent of the γ-deformation. For the ground states of these nuclei one finds pronounced discontinuities in the

relative fluctuations of the quadrupole deformations $\Delta\beta/\langle\beta\rangle$ and $\Delta\gamma/\langle\gamma\rangle$. The calculated spectra are remarkably similar to the level schemes predicted by the $E(5)$ dynamical symmetry model and, therefore, display fingerprints of a second-order shape phase transition.

The fact that the same microscopic model describes both first- and second-order QPTs in different mass regions is, in our opinion, an interesting result that illustrates the importance of microscopic studies of QPT starting from nucleonic degrees of freedom. A quantitative comparison with experimental spectra, particularly with very recent data for ^{128}Xe, points to some intrinsic problems in the description of excited 0^+ states and clearly indicates that one must go beyond the simple cranking approximation for the model mass parameters (vibrational inertial functions) or even extend the model by explicitly taking into account the coupling of nuclear shape oscillations with pairing vibrations.

ACKNOWLEDGMENTS

We thank R. F. Casten, F. Iachello, and P. Ring for useful discussions. This work was supported in part by MZOS Project No. 1191005-1010, by the Major State 973 Program 2007CB815000, and by the NSFC under Grant Nos.10775004 and 10975008. The work of J.M, T.N., and D.V. was supported in part by the Chinese-Croatian project "Nuclear Structure and Astrophysical Applications." T.N. and Z.P. Li acknowledge support by the Croatian National Foundation for Science, Higher Education and Technological Development.

[1] F. Iachello, in *Proceedings of the International School of Physics "Enrico Fermi" Course CLIII*, edited by A. Molinari, L. Riccati, W. M. Alberico, and M. Morando (IOS Press, Amsterdam, 2003).
[2] J. Jolie and R. F. Casten, Nucl. Phys. News. **15**, 20 (2005).
[3] R. F. Casten, Nature Phys. **2**, 811 (2006).
[4] R. F. Casten and E. A. McCutchan, J. Phys. G **34**, R285 (2007).
[5] P. Cejnar and J. Jolie, Prog. Part. Nucl. Phys. **62**, 210 (2009).
[6] D. Bonatsos, in *Proceedings of the 24th International Physics Congress of the Turkish Physical Society (Malatya, 2007)*, arXiv:0807.4492[nucl-th],
[7] F. Iachello, Phys. Rev. Lett. **85**, 3580 (2000).
[8] R. F. Casten and N. V. Zamfir, Phys. Rev. Lett. **85**, 3584 (2000).
[9] F. Iachello, Phys. Rev. Lett. **87**, 052502 (2001).
[10] R. F. Casten and N. V. Zamfir, Phys. Rev. Lett. **87**, 052503 (2001).
[11] F. Iachello and A. Arima, *The Interacting Boson Model* (Cambridge University Press, Cambridge, 1987).
[12] J. Meng, W. Zhang, S. G. Zhou, H. Toki, and L. S. Geng, Eur. Phys. J. A **25**, 23 (2005).
[13] Z.-Q. Sheng and J.-Y. Guo, Mod. Phys. Lett. A **20**, 2711 (2005).
[14] R. Fossion, D. Bonatsos, and G. A. Lalazissis, Phys. Rev. C **73**, 044310 (2006).
[15] T. Nikšić, D. Vretenar, G. A. Lalazissis, and P. Ring, Phys. Rev. Lett. **99**, 092502 (2007).
[16] R. Rodríguez-Guzmán and P. Sarriguren, Phys. Rev. C **76**, 064303 (2007).
[17] T. R. Rodríguez and J. L. Egido, Phys. Lett. B **663**, 49 (2008).
[18] L. M. Robledo, R. R. Rodríguez-Guzmán, and P. Sarriguren, Phys. Rev. C **78**, 034314 (2008).
[19] Z. P. Li, T. Nikšić, D. Vretenar, J. Meng, G. A. Lalazissis, and P. Ring, Phys. Rev. C **79**, 054301 (2009).
[20] Z. P. Li, T. Nikšić, D. Vretenar, and J. Meng, Phys. Rev. C **80**, 061301(R) (2009).
[21] T. Nikšić, Z. P. Li, D. Vretenar, L. Próchniak, J. Meng, and P. Ring, Phys. Rev. C **79**, 034303 (2009).
[22] T. Bürvenich, D. G. Madland, J. A. Maruhn, and P.-G. Reinhard, Phys. Rev. C **65**, 044308 (2002).
[23] P. Ring and P. Schuck, *The Nuclear Many-Body Problem* (Springer-Verlag, Heidelberg, 1980).
[24] NNDC National Nuclear Data Center, Brookhaven National Laboratory; http://www.nndc.bnl.gov/.
[25] LBNL Isotopes Project Nuclear Data Dissemination Home Page, http://ie.lbl.gov/toi.html.
[26] J. Srebrny *et al.*, Nucl. Phys. A **766**, 25 (2006).
[27] A. M. Kleinfeld, A. Bockisch, and K. P. Lieb, Nucl. Phys. A **283**, 526 (1977).
[28] S. M. Burnett *et al.*, Nucl. Phys. A **432**, 514 (1985).
[29] J. Libert, M. Girod, and J.-P. Delaroche, Phys. Rev. C **60**, 054301 (1999).
[30] G. Jakob *et al.*, Phys. Rev. C **65**, 024316 (2002).
[31] R. M. Clark *et al.*, Phys. Rev. C **69**, 064322 (2004).
[32] D. Bonatsos, D. Lenis, N. Pietralla, and P. A. Terziev, Phys. Rev. C **74**, 044306 (2006).
[33] N. Pietralla and O. M. Gorbachenko, Phys. Rev. C **70**, 011304(R) (2004).
[34] L. Coquard *et al.*, Phys. Rev. C **80**, 061304(R) (2009).
[35] L. Próchniak, P. Quentin, D. Samsoen, and J. Libert, Nucl. Phys. A **730**, 59 (2004).
[36] L. Próchniak and S. G. Rohoziński, J. Phys. G **36**, 123101 (2009).
[37] S. Pilat and K. Pomorski, Nucl. Phys. A **554**, 413 (1993).
[38] S. G. Rohoziński, J. Dobaczewski, B. Nerlo-Pomorska, K. Pomorski, and J. Srebrny, Nucl. Phys. A **292**, 66 (1977).
[39] J.-P. Delaroche, M. Girod, J. Libert, H. Goutte, S. Hilaire, S. Péru, N. Pillet, and G. F. Bertsch, Phys. Rev. C **81**, 014303 (2010).